China Geology 1 (2020) 113−123

China Geology

Journal homepage: http://chinageology.cgs.cn
https://www.sciencedirect.com/journal/china-geology

Soil water movement and deep drainage through thick vadose zones on the northern slope of the Tianshan Mountain: Croplands *vs.* natural lands

Fang-qiang Sun[a], Li-he Yin[a,*], Wu-hui Jia[b], Jun Zhang[a], Xiao-yong Wang[a], Li-feng Zhu[a], Xin-xin Zhang[c], Xiao-ping Tang[a], Jia-qiu Dong[a]

[a] *Xi'an Center of Geological Survey, China Geological Survey, Ministry of Natural Resources, Xi'an* 710054, *China*
[b] *School of Water Resources and Environment, China University of Geosciences, Beijing* 100083, *China*
[c] *Chinese Academy of Geological Sciences, China Geological Survey, Ministry of Natural Resources, Beijing* 100037, *China*

ARTICLE INFO

Article history:
Received 12 December 2019
Received in revised form 8 February 2020
Accepted 13 March 2020
Available online 16 March 2020

Keywords:
Land-use
Soil water
Groundwater recharge
Deep drainage
Unsaturated zone
Arid regions
Cropland
Natural land
Groundwater survey engineering
Tianshan Mountain
China

ABSTRACT

Regional aridity is increasing under global climate change, and therefore the sustainable use of water resources has drawn attention from scientists and the public. Land-use changes can have a significant impact on groundwater recharge in arid regions, and quantitative assessment of the impact is key to sustainable groundwater resources management. In this study, the changes of groundwater recharge after the conversion of natural lands to croplands were investigated and compared in inland and arid region, i.e., the northern slope of the Tianshan Mountain. Stable isotopes suggest that soil water in topsoil (< 2 m) has experienced stronger evaporation under natural lands than croplands, and then moves downward as a piston flow. Recharge was estimated by the tracer-based mass balance method, i.e., chloride and sulfate. Recharge rates under natural conditions estimated by the chloride mass balance (CMB) method were estimated to be 0.07 mm/a in deserts and 0.4 mm/a in oases. In contrast, the estimated groundwater recharge ranged from 61.2 mm/a to 44.8 mm/a in croplands, indicating that groundwater recharge would increase significantly after land changes from natural lands to irrigated croplands in arid regions. Recharge estimated by the sulfate mass balance method is consistent with that from the CMB method, indicating that sulfate is also a good tracer capable of estimating groundwater recharge.

1. Introduction

Regional aridity is increasing under global climate change, and therefore the sustainable use of water resources has drawn attention from scientists and the public (Yin LH et al., 2015; Zhang GF et al., 2003). In arid regions, groundwater is the main source of water supply for urban, industrial and agricultural development due to unreliability and over-allocation of surface water (Simmers I, 2013). Due to unsustainable development, groundwater depletion has taken place widely in large-scale regional aquifers (Scanlon BR et al., 2012; Feng W et al., 2013; Doell P et al., 2014). Groundwater recharge/percolation, therefore, is essential to the sustainable use of groundwater, particularly in arid regions (Scanlon BR et al., 2006; Huang TM, et al., 2017). Percolation is defined as water movement below the root zone, whereas recharge is used to describe water that reaches the water table. However, the two terms are often equated to each other (Scanlon BR et al., 2002). Although many methods are available to estimate groundwater recharge/percolation, for example, Water-balance Methods, Empirical Formulae, Isotope-tracer Techniques, and Darcian Approaches, quantification of recharge fluxes in arid regions remains challenging due to the complex process, the strong spatial and temporal variations and the preferential flow (Yin LH et al., 2011; Federico AF and Geoff P, 2010).

Among the existing methods, Tracer Methods are effective and have the best potential for reliable point estimation of groundwater recharge in arid regions where groundwater recharge is very low, i.e., less than 1 mm/a in extreme cases (Scanlon BR et al., 2002; Chen ZY et al., 2001; Chen ZY et al., 1998; Cook PG et al., 1992). The most commonly used tracer-based method is the chloride mass balance (CMB) method because of its low cost and time integrating properties (Wood WW, 1999; Chen Z and Xu H,

* Corresponding author: *E-mail address*: ylihe@cgs.cn (Li-he Yin).

doi:10.31035/cg2020008
2096-5192/© 2020 China Geology Editorial Office.

1996; Liu XY et al., 2010), requiring only information of chloride in precipitation, groundwater or soil water (Crosbie RS et al., 2017; Perera N et al., 2013; Russo SL et al., 2003). The application of the CMB method can be traced back in the 1940s (Anderson VG, 1945), and it has been widely used since then in (semi-) arid regions, including USA (Tyler SW et al, 1996; Scanlon BR et al, 2007), Australia (Stone WJ, 1992; Harrington GA, et al., 2002; Tolmie PE et al., 2011) and China (Gates JB et al., 2008b). Other tracers, such as sulfate (SO_4) and fluoride, have also been used to estimate groundwater recharge in limited cases (Scanlon BR et al., 2006; Adane ZA and Gates JB, 2015), providing that they are not absorbed by soils. However, the applicability of these ions to estimate groundwater recharge needs more cases to validate and groundwater recharge estimated by two tracer-based methods is seldom compared.

Land-use changes have significant impacts on groundwater recharge as indicated by previous studies (Allison GB and Hughes MW, 1983; Cook PG et al., 2001) as vegetation changes associated with land-use alternation ranks the second controlling factor on groundwater recharge (Wang YG et al., 1993; Kim JH and Jackson RB, 2012; Wang Q et al., 2013). The most common land-use change is the conversion of natural lands for agriculture that has been practiced worldwide to meet the increasing food demand (Tilman D et al., 2011; Ma QL et al., 2009; Schmidt S et al., 2013), which has a substantial impact on groundwater recharge (Scanlon BR et al., 2005). The previous studies indicate that land-clearing for the crop has increased groundwater recharge in order of magnitude (Allison GB and Hughes RW, 1983; Han D et al., 2017). Since the 1950s, croplands in arid northwestern China have expanded remarkably to provide sufficient food production and to promote economic growth. In these areas, croplands have increased by 4800 km^2 from 1987 to 2000 according to the study on land-use change by remote sensing (Yan HM et al., 2009) and keep increasing after 2000 when other areas in China are experiencing reduction with respect to cropland areas (Zhang ZH et al., 1997; Zuo LJ et al., 2018). In some specific sites, the rate of cropland increase is even faster. In an inland arid Heihe River Basin, the results show that the cultivated croplands along oasis fringes increased by 15.38% and 43.60% during the period of 1965–1986 and 1986–2007, respectively (Nian YY et al., 2014). Several studies on the impact of land-use changes on groundwater recharge have been conducted in (semi-) arid regions (Wang BG et al., 2006; Zhu GF et al., 2007; Huang TM et al. 2017). However considering the vast area of NW China (about 3.3×10^6 km^2) with various climate, soil, and vegetation, quantitative assessments on the impact by previous studies are still inadequate.

In this study, the northern slope of the Tianshan Mountain in NW China was selected as the study area where soil profiles were excavated in natural and agricultural lands and groundwater recharge was estimated based on the chloride- and sulfate-based tracer methods. The main objectives are: (1) To quantify groundwater recharge under different land use; (2) To compare the changes after the conversion from natural lands to croplands; and (3) To validate the applicability of the sulfate-based tracer method to quantify groundwater recharge.

2. Materials and methods

2.1. Study area

The study site is located on the northern slope of the Tianshan Mountain, covering an area of about 2300 km^2. The southern study area is a mountainous region (800−4000 m above sea level), the middle region is covered by oases (450−500 m above sea level) and the northern part is characterized by a desert landscape (440−460 m above sea level) (Fig. 1). Mean annual precipitation varies between 220 mm (M1 station, 1961−2014 from http://data.cma.cn/) and 173 mm (M2 station, 2006−2015 from the local meteorological Bureau) (Fig. 2). The majority of rainfall (about 64%) occurs in the period April through September, mainly in a form of thunderstorm. Air temperature ranges from 26.1℃ in July to –19.1℃ in January, with a mean value of 7.0℃ at M1 station. Potential evapotranspiration at M1 station is about 1960 mm/a, exceeding annual precipitation greatly.

Land-use is mainly natural grasslands and shrublands (47%), croplands (33%), and water bodies and cities (10% in total) (Zhang Q et al., 2017). Croplands are mainly irrigated by groundwater due to the scarcity of precipitation and surface water resources and cover an area of about 200 km^2. Flooding irrigation was mainly used at the early land development stage and has been converted to dipping irrigation recently for water-saving. The thickness of the vadose zone is higher in the mountainous areas (about 70 m) and lower in the oasis and desert (about 5−10 m). Groundwater is mainly stored in Quaternary unconsolidated porous aquifers and flows toward the north. Groundwater quality is good with total dissolved solids ranging from 500 mg/L to 1000 mg/L.

Precipitation chemistry is monitored by China Acid Deposition Monitoring Network (Fig. 3). The nearest monitoring station is in Urumqi (about 60 km northwest of the study area) where long-term data of wet-only deposition are available for 11 years (1999−2009) (Fig. 3). Volume-weighted mean wet annual chloride $(Cl)^-$ and SO_4^{2-} concentrations are 8.8 mg/L and 30.4 mg/L, respectively.

2.2. Field sampling and laboratory methods

Four pits (Fig. 1), two under irrigated croplands and two under natural lands, were dug into a depth ranging from 5.7 m to >9 m (Table 1) and a direct push rig was used to take soil core samples at 0.2 m intervals. TP1 and TP2 are in natural lands, one in oasis partially covered by grass and the other in the desert without any vegetation on the surface. TP3 and TP4 are in croplands with melon and sunflower, respectively. The amount of flooding irrigation is about 620 mm/a and 675 mm/a at TP3 and TP4, respectively (Local Statistical Bureau) and Cl^- concentration in irrigation water is 21 mg/L and 33 mg/L

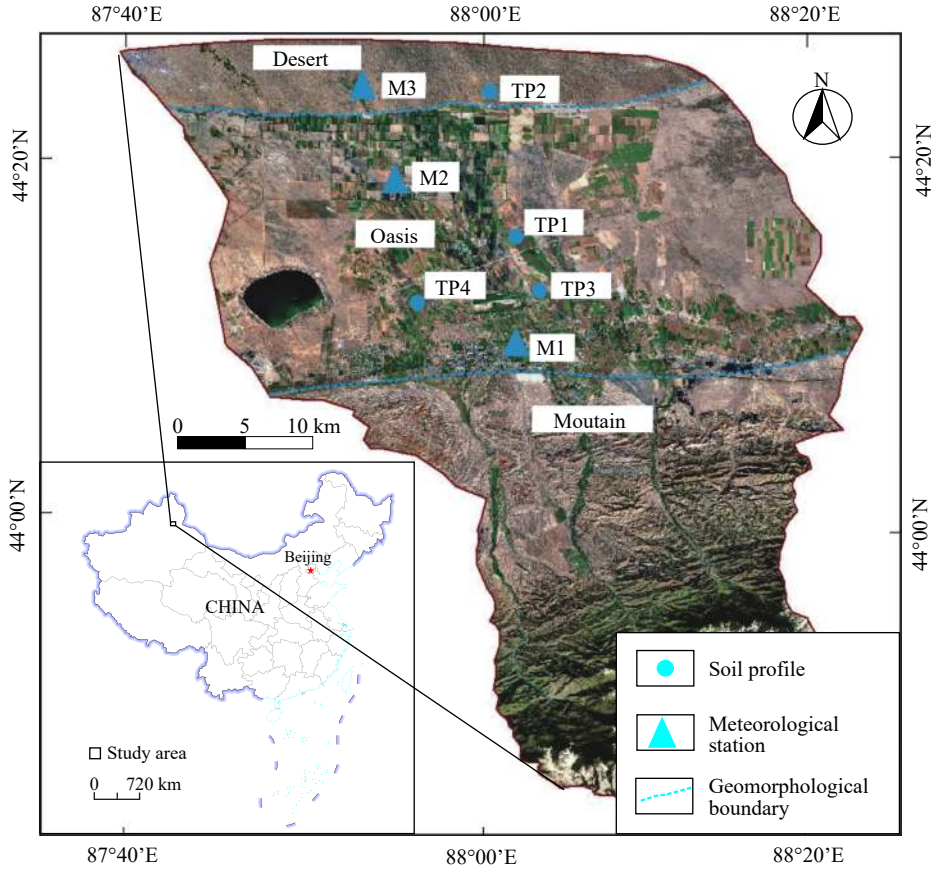

Fig. 1. Location of the study area, showing the major landscapes, sampled profiles and meteorological stations.

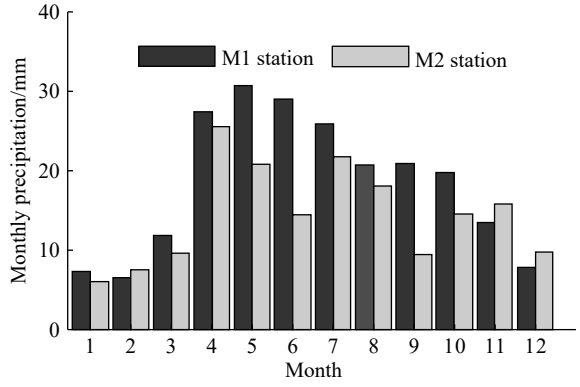

Fig. 2. Averaged monthly precipitation from long-term data (M1, 1961−2014; M2, 2006−2015).

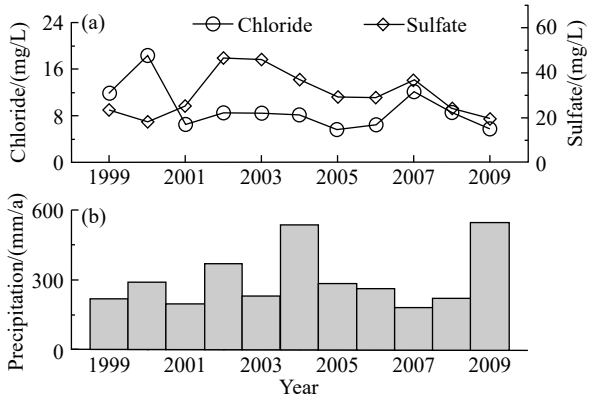

Fig. 3. Yearly chloride, sulfate in precipitation during 1999−2009 (a) and yearly precipitation during 1999−2009 (b).

at TP3 and TP4, respectively.

The samples were sectioned for the analyses of particle size, soil moisture, chloride and stable water isotopes. Particle-size distributions were determined by the sieving method for the sand fractions and by a soil hydrometer for the silt and clay fractions. Gravimetric soil water content was determined by weighing before and after oven-drying at 105℃. Chloride concentration in soil water was analyzed in water leached from soil samples. About 40 mL of double deionized water was added to 25 g of soil and the mixture was shaken for 4 h, centrifuged at 7000 rpm for 30 min until the visible separation of soil and water, and finally filtered. Cl^- and SO_4^{2-} concentrations were measured by ion chromatography (Dionex ICS-1100, Thermo Fisher Scientific Inc.), and were expressed on a mass basis and then were converted to mg/L by dividing gravimetric water content and multiplying by water density. Soil water was extracted by the high-temperature vacuum distillation method using a LI-2000 soil water extractor (Lijia Scientific instrument Inc., China). ^{18}O and ^{2}H were measured by a cavity ring-down spectrometer (L1102-i, Picarro, Inc., CA, USA) and were expressed in δ-notation with respect to VSMOW (Vienna Standard Mean Ocean Water).

2.3. Data analysis

The CMB method has been widely applied to estimate deep drainage (Huang TM et al., 2011). The basic

Table 1. Locations, vegetation type, depth and sampling information of profiles.

Profile	Vegetation type	Longitude	Latitude	Elevation/m	Core depth/m	Numbers of samples	Water table depth/m
TP1	Grass	E88°05'18"	N44°15'56"	498	5.8	29	5.9
TP2	/	E88°04'39"	N44°21'5"	472	8.8	44	>9.0
TP3	Melon	E88°05'44"	N44°12'58"	508	6.4	32	6.5
TP4	Sunflower	E87°57'39"	N44°11'58"	511	5.7	29	5.8

Note: Data from the laboratory of Xi'an Center of China Geological Survey.

assumptions of the method are as follows: (1) Chloride is conservative; (2) Atmospheric input is assumed to be constant with time; and (3) Water movement in thick vadose zones is vertically non-diffusive below the root zone. Surface runoff was ignored due to the low precipitation in the study area. In natural systems, the CMB method was used to determine deep drainage (D) as follows:

$$D = \frac{P \times Cl_p + D_c}{Cl_{uz}} \quad (1)$$

where P is the annual precipitation (mm/a), Cl_p is the Cl^- concentration in precipitation (mg/L), Cl_{uz} is the Cl^- concentration in soil water (mg/L) and D_c is the dry deposition of chloride from other sources. The value of dry deposition is from the previous study with a similar environmental condition, reporting that the annual dry depositions for croplands and natural lands were about 0.66 g/m^2 and 1.16 g/m^2, respectively (Zhang N et al., 1999). When the CMB method is applied in irrigated lands, irrigation rate (I, mm/a) and Cl^- concentration in irrigation water (Cl_I) must be included as following:

$$D = \frac{P \times Cl_p + I \times Cl_I}{Cl_{uz}} \quad (2)$$

The principal of the mass balance method can be applied to other elements if the input of a tracer can be quantified and the tracer behaves conservatively (Scanlon BR et al., 2002). In this study, SO_4^{2-} was also used to estimate deep drainage, assuming no subsurface sources or sinks for SO_4^{2-}, but the dry deposition of SO_4^{2-} was ignored as no such data were available for the study area. Due to the possible existence of plant and microbial SO_4^{2-} uptake (Taiz L and Zeiger E, 2010), the water washing coefficient (WWC) was calculated to valid the no sink assumption by Eq. 3 as following:

$$WWC_i = \frac{c_{i-1}}{c_i} \quad (3)$$

where WWC_i is the water washing coefficient in the ith layer (-), c_{i-1} (mg/L) and c_i (mg/L) are the concentration of a tracer in layer i-1 and i, respectively. If WWC indicates that the adsorption of SO_4^{2-} is negligible, then a similar equation to Eq. 1 and Eq. 2 can be written for the SO_4^{2-}-based deep drainage estimation.

By assuming a constant atmospheric input, the time required to accumulate a certain amount of Cl^- in a profile (t) was determined by dividing the total mass of Cl^- to the depth of the profile (Selaolo ET, 1998):

$$t = \int_0^z \theta Cl_{uz} dz / \left(P \times Cl_p\right) \quad (4)$$

where θ is soil water content (cm^3/cm^3). Eq. 4 assumes a constant Cl^- input from precipitation, which is supported by $^{36}Cl/Cl^-$ ratios in other sites (Scanlon BR et al., 2002). A similar equation can be used to calculate the accumulated age for the cropland profiles under the consumption of constant inputs from the atmosphere and irrigation.

3. Results and discussion

3.1. Stable-isotope profiles

The depth profiles of $\delta^{18}O$ and δD of soil water are shown in Fig. 4. All profiles show strong enrichment at the top 2 m, indicating a strong evaporation loss from the top surface under high evaporation demand in arid regions (Torres EA and Calera A, 2010). The mean values of $\delta^{18}O$ were –6.2‰ and –7.7‰ at TP1 and TP2, respectively, higher than the values in the croplands (–10.7‰ and –13.0‰ for TP3 and TP4, respectively). The more enriched signature implied that soil water suffered stronger evaporation at natural conditions than croplands. Beneath 2 m, the variation of $\delta^{18}O$ and δD was narrow, less than 5‰ in $\delta^{18}O$ and 20‰ in δD (Table 2; Fig. 4), suggesting a uniform piston flow.

Compared to the local meteoric water line (LMWL) (Wei J et al. 2011), the slope of the vadose zone water line is lower than that of LMWL (about 7.2) (Table 3; Fig. 5). The slopes for TP1 and TP2 are similar, being 3.3 and 3.2 respectively (Table 3; Fig. 5). The slopes for the profiles in croplands are slightly higher than that in natural lands (4.8 and 4.3 for TP3 and TP4, respectively) (Table 3; Fig. 5). The lower values of the slope in natural lands indicate that stronger evaporation is present, which agrees with the inference from the depth profiles of $\delta^{18}O$ and δD.

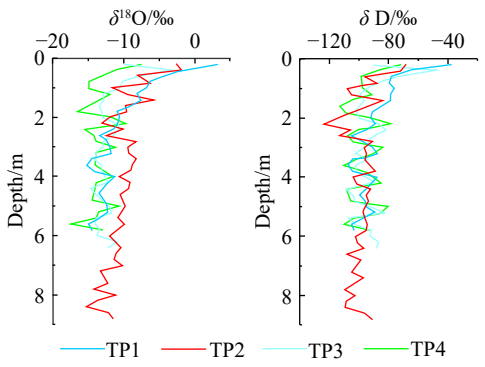

Fig. 4. Depth profiles of $\delta^{18}O$ and δD of soil water.

Table 2. $\delta^{18}O$ and δD of soil water at different depths.

	$\delta^{18}O$								δD							
Depth/m	TP1	Depth/m	TP2	Depth/m	TP3	Depth/m	TP4	Depth/m	TP1	Depth/m	TP2	Depth/m	TP3	Depth/m	TP4
0.2	3.18	0.2	–2.54	0.2	–9.88	0.1	–7.52	0.2	–37.83	0.2	–68.34	0.2	–90.08	0.1	–71.77
0.4	–1.66	0.4	–1.77	0.4	–3.26	0.3	–11.14	0.4	–68.04	0.4	–72.03	0.4	–46.50	0.3	–87.97
0.6	–4.53	0.6	–8.19	0.6	–7.79	0.5	–12.70	0.6	–78.37	0.6	–96.50	0.6	–75.06	0.5	–98.64
0.8	–6.36	0.8	–6.29	0.8	–10.16	0.7	–14.92	0.8	–79.58	0.8	–87.22	0.8	–88.11	0.7	–98.03
1	–6.73	1	–11.59	1	–10.51	0.9	–14.91	1.0	–76.34	1.0	–108.31	1.0	–94.37	0.9	–97.57
1.2	–8.13	1.2	–9.67	1.2	–12.85	1.1	–11.86	1.2	–78.61	1.2	–105.06	1.2	–99.55	1.1	–91.68
1.4	–7.49	1.4	–5.67	1.4	–12.79	1.3	–13.79	1.4	–78.51	1.4	–82.79	1.4	–96.10	1.3	–105.33
1.6	–9.10	1.6	–9.86	1.6	–13.41	1.5	–15.19	1.6	–85.65	1.6	–95.47	1.6	–99.96	1.5	–112.93
1.8	–11.01	1.8	–9.53	1.8	–13.06	1.7	–16.61	1.8	–91.34	1.8	–103.69	1.8	–103.33	1.7	–108.86
2	–10.59	2	–11.89	2	–12.90	1.9	–11.25	2.0	–92.24	2.0	–115.57	2.0	–99.59	1.9	–91.89
2.2	–10.79	2.2	–13.07	2.2	–10.64	2.1	–9.56	2.2	–88.59	2.2	–124.10	2.2	–85.76	2.1	–77.21
2.4	–11.42	2.4	–10.03	2.4	–10.65	2.3	–15.54	2.4	–94.96	2.4	–104.59	2.4	–81.60	2.3	–100.39
2.6	–13.44	2.6	–12.53	2.6	–11.47	2.5	–14.23	2.6	–105.78	2.6	–114.06	2.6	–89.40	2.5	–107.72
2.8	–12.24	2.8	–8.16	2.8	–12.81	2.7	–13.78	2.8	–97.37	2.8	–89.83	2.8	–94.49	2.7	–104.02
3	–11.88	3	–9.41	3	–12.96	2.9	–11.07	3.0	–89.79	3.0	–96.45	3.0	–96.59	2.9	–83.68
3.2	–11.67	3.2	–9.33	3.2	–13.94	3.1	–13.88	3.2	–87.26	3.2	–94.99	3.2	–102.61	3.1	–89.91
3.4	–14.69	3.4	–8.22	3.4	–14.00	3.3	–14.00	3.4	–104.18	3.4	–96.18	3.4	–94.11	3.3	–102.57
3.6	–15.25	3.6	–8.76	3.6	–13.29	3.5	–13.96	3.6	–107.56	3.6	–92.32	3.6	–102.58	3.5	–110.47
3.8	–14.10	3.8	–9.03	3.8	–12.99	3.7	–12.50	3.8	–104.31	3.8	–88.75	3.8	–101.63	3.7	–96.10
4	–11.28	4	–10.68	4	–12.62	3.9	–11.41	4.0	–87.24	4.0	–104.77	4.0	–95.04	3.9	–89.89
4.2	–12.32	4.2	–9.03	4.2	–12.20	4.1	–13.89	4.2	–92.19	4.2	–102.19	4.2	–88.46	4.1	–84.39
4.4	–12.86	4.4	–9.32	4.4	–14.73	4.3	–13.91	4.4	–94.96	4.4	–92.00	4.4	–108.40	4.3	–108.65
4.6	–13.63	4.6	–10.50	4.6	–13.52	4.5	–14.35	4.6	–99.77	4.6	–95.40	4.6	–103.84	4.5	–106.96
4.8	–12.83	4.8	–10.15	4.8	–13.08	4.7	–14.46	4.8	–95.96	4.8	–93.75	4.8	–102.48	4.7	–106.05
5	–12.34	5	–9.77	5	–11.95	4.9	–10.46	5.0	–94.69	5.0	–96.09	5.0	–92.47	4.9	–80.20
5.2	–12.16	5.2	–10.44	5.2	–11.61	5.1	–13.61	5.2	–88.65	5.2	–97.39	5.2	–82.63	5.1	–84.93
5.4	–13.55	5.4	–10.86	5.4	–13.90	5.3	–13.90	5.4	–97.44	5.4	–95.88	5.4	–107.26	5.3	–103.76
5.6	–14.97	5.6	–9.91	5.6	–14.01	5.5	–17.38	5.6	–105.54	5.6	–94.42	5.6	–102.68	5.5	–110.91
5.8	–14.42	5.8	–11.01	5.8	–13.36	5.7	–12.91	5.8	–102.95	5.8	–95.10	5.8	–91.56	5.7	–92.57
		6	–12.04	6	–13.75					6.0	–102.84	6.0	–92.35		
		6.2	–11.15	6.2	–10.81					6.2	–101.43	6.2	–86.39		
		6.4	–10.36	6.4	–12.24					6.4	–96.19	6.4	–88.13		
		6.6	–11.04							6.6	–109.10				
		6.8	–11.36							6.8	–98.40				
		7	–10.11							7.0	–102.30				
		7.2	–13.26							7.2	–105.29				
		7.4	–12.48							7.4	–96.44				
		7.6	–12.17							7.6	–102.46				
		7.8	–14.19							7.8	–110.15				
		8	–10.99							8.0	–102.28				
		8.2	–13.94							8.2	–108.93				
		8.4	–15.23							8.4	–109.79				
		8.6	–12.01							8.6	–96.24				
		8.8	–11.46							8.8	–91.14				

3.2. Soil profiles under natural conditions

Soil water contents (SWCs) in the oasis profile (TP1) fluctuated at a range of 10%−20% within 0−4 m, increased gradually from 20% to 35% below 4 m (Fig. 6a). The elevated soil water contents at TP1 near the bottom attributed to the capillary rise of water table where the depth to water table was about 6 m. In contrast, the top soil water contents at TP2 in the desert were similar to TP1, but soil water contents below 4 m were generally lower than 10% (Fig. 6a). The mean SWCs were 18.7% and 7.7% at TP1 and TP2 (Table 4), respectively, indicating that soil water was less in the desert due to the drier conditions and less precipitation.

In the oasis, Cl^- concentrations ranged from 4279.2 mg/L to 24354.5 mg/L with a mean value of 9169.3 mg/L (Table 4), and the peak value occurred at about 0.6 m depth (Fig. 6b). In the desert, the Cl^- concentrations varied between 14548.5 mg/L and 64989.1 mg/L with a mean value of 33904.7 mg/L, and

Table 3. $\delta^{18}O$ and δD of soil water for TP1, TP2, TP3 and TP4.

TP1		TP2		TP3		TP4	
$\delta^{18}O$	δD	$\delta^{18}O$	δD	$\delta^{18}O$	δD	$\delta^{18}O$	δD
3.18	–37.83	–2.54	–68.34	–9.88	–90.08	–7.52	–71.77
–1.66	–68.04	–1.77	–72.03	–3.26	–46.50	–11.14	–87.97
–4.53	–78.37	–8.19	–96.50	–7.79	–75.06	–12.70	–98.64
–6.36	–79.58	–6.29	–87.22	–10.16	–88.11	–14.92	–98.03
–6.73	–76.34	–11.59	–108.31	–10.51	–94.37	–14.91	–97.57
–8.13	–78.61	–9.67	–105.06	–12.85	–99.55	–11.86	–91.68
–7.49	–78.51	–5.67	–82.79	–12.79	–96.10	–13.79	–105.33
–9.10	–85.65	–9.86	–95.47	–13.41	–99.96	–15.19	–112.93
–11.01	–91.34	–9.53	–103.69	–13.06	–103.33	–16.61	–108.86
–10.59	–92.24	–11.89	–115.57	–12.90	–99.59	–11.25	–91.89
–10.79	–88.59	–13.07	–124.10	–10.64	–85.76	–9.56	–77.21
–11.42	–94.96	–10.03	–104.59	–10.65	–81.60	–15.54	–100.39
–13.44	–105.78	–12.53	–114.06	–11.47	–89.40	–14.23	–107.72
–12.24	–97.37	–8.16	–89.83	–12.81	–94.49	–13.78	–104.02
–11.88	–89.79	–9.41	–96.45	–12.96	–96.59	–11.07	–83.68
–11.67	–87.26	–9.33	–94.99	–13.94	–102.61	–13.88	–89.91
–14.69	–104.18	–8.22	–96.18	–14.00	–94.11	–14.00	–102.57
–15.25	–107.56	–8.76	–92.32	–13.29	–102.58	–13.96	–110.47
–14.10	–104.31	–9.03	–88.75	–12.99	–101.63	–12.50	–96.10
–11.28	–87.24	–10.68	–104.77	–12.62	–95.04	–11.41	–89.89
–12.32	–92.19	–9.03	–102.19	–12.20	–88.46	–13.89	–84.39
–12.86	–94.96	–9.32	–92.00	–14.73	–108.40	–13.91	–108.65
–13.63	–99.77	–10.50	–95.40	–13.52	–103.84	–14.35	–106.96
–12.83	–95.96	–10.15	–93.75	–13.08	–102.48	–14.46	–106.05
–12.34	–94.69	–9.77	–96.09	–11.95	–92.47	–10.46	–80.20
–12.16	–88.65	–10.44	–97.39	–11.61	–82.63	–13.61	–84.93
–13.55	–97.44	–10.86	–95.88	–13.90	–107.26	–13.90	–103.76
–14.97	–105.54	–9.91	–94.42	–14.01	–102.68	–17.38	–110.91
–14.42	–102.95	–11.01	–95.10	–13.36	–91.56	–12.91	–92.57
		–12.04	–102.84	–13.75	–92.35		
		–11.15	–101.43	–10.81	–86.39		
		–10.36	–96.19	–12.24	–88.13		
		–11.04	–109.10				
		–11.36	–98.40				
		–10.11	–102.30				
		–13.26	–105.29				
		–12.48	–96.44				
		–12.17	–102.46				
		–14.19	–110.15				
		–10.99	–102.28				
		–13.94	–108.93				
		–15.23	–109.79				
		–12.01	–96.24				
		–11.46	–91.14				

the Cl^- contents of soil water were highest near the land surface at around 65000 mg/L. The total amount of accumulated Cl^- over the entire profile of TP1 was equivalent to about 3500 years of rainfall Cl^- input. In contrast, the total amount of accumulated Cl^- in TP2 equaled to 10300 years of atmospheric deposition. Thus, the two profiles contain long records of climatic variation as seen in other dry sites (Radford BJ et al., 2009; Scanlon BR et al., 2007). The deep drainage under natural vegetation was low, ranging from 0.07 mm/a in the desert to 0.4 mm/a in the oasis from the CMB method.

WWCs of SO_4^{2-} did not decrease with depth, indicating that SO_4^{2-} was not absorbed by the soil (Fig. 7). Therefore, deep drainage was also estimated by the sulfate mass balance (SMB) method. In the oasis, SO_4^{2-} ranged from 11004.1 mg/L to 175435.4 mg/L with a mean value of 46907.6 mg/L (Fig. 6c). In the desert, SO_4^{2-} concentrations fluctuated significantly at the top 2 m, and then became stable. The deep drainage from the SMB method varied between 0.16 mm/a in the desert and 0.3 mm/a in the oasis. The deep drainage estimated by SO_4^{2-} is generally consistent with the chloride-based estimation, suggesting that the SMB method can be used to estimated deep drainage at a relatively high precision (Scanlon BR et al., 2010).

3.3. Soil profiles under croplands

Soil water contents along the two cropland profiles were similar, showing a fluctuation with depth, but generally increased with depth (Fig. 8a). The mean soil water contents were 17.9% and 22.4% for TP3 and TP4, respectively. Soil water Cl^- contents of the two profiles followed a similar pattern, showing an increase from the surface and reaching the maximum of about 1000 mg/L and then decreasing and being stable at 2−3 m (Fig. 8b). The mean Cl^- contents at TP3 and TP4 were 300.9 mg/L and 457.4 mg/L, respectively, much lower than that in natural lands. Based on Eq. 2, the deep drainage under croplands ranged from 61.2 mm/a in TP3 to 44.8 mm/a in TP4.

The concentrations of SO_4^{2-} at the two profiles generally decreased with depth and reached stable values at 2−3 m depth (Fig. 8c). The deep drainage under croplands ranged from 95.6 mm/a in TP3 to 24.5 mm/a in TP4 by the SMB method, which was consistent with the results from the CMB method. The use of SO_4^{2-} to estimate groundwater recharge is uncommon and only three cases were reported in the USA and China (Scanlon BR et al., 2006; Adane ZA and Gates JB, 2015). This study further indicates that SO_4^{2-} has promise as an independent check on the results from the CMB method and can be used at natural lands and croplands.

3.4. Comparison with other studies

Deep drainage rates usually do not exceed 3 mm/a at natural conditions in arid regions of Northwest China (Ma JZ et al., 2005, 2009b; Edmunds WM et al., 2006; Gates JB et al., 2008b). For example, the mean recharge under 18 unsaturated zone profiles in the Badain Jaran Desert in NW China is 1.4 mm/a (Gates JB et al., 2008a), and groundwater recharge ranges from 0.9 mm/a to 2.5 mm/a in the eastern part of the Hexi Corridor and western part of the Tengger Desert (Ma JZ et al., 2009a). Besides China, in Australia, the United States and Africa, many studies have shown that under natural ecosystems groundwater recharge is little or no recharge (Scanlon BR et al., 2007). These studies, in general, have a good agreement with this study. However recharge at TP2 is

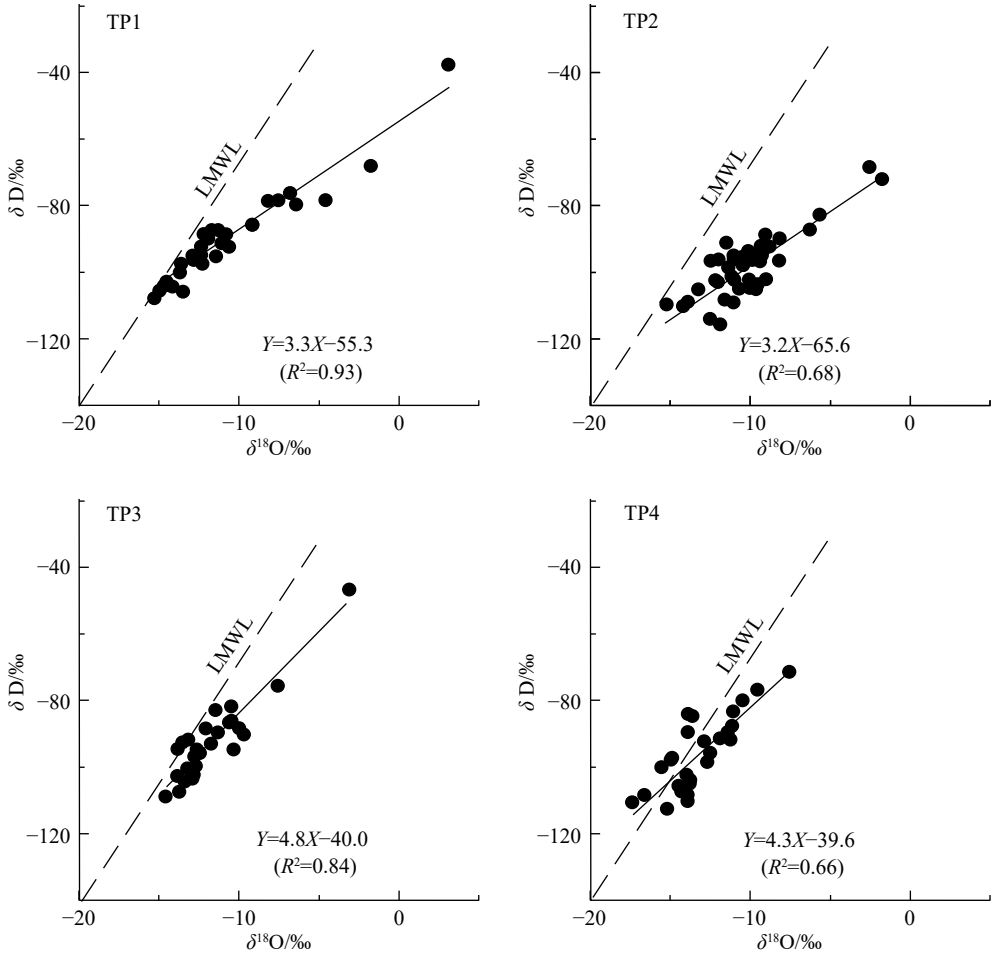

Fig. 5. Relationship between $\delta^{18}O$ and δD of soil water for the four profiles.

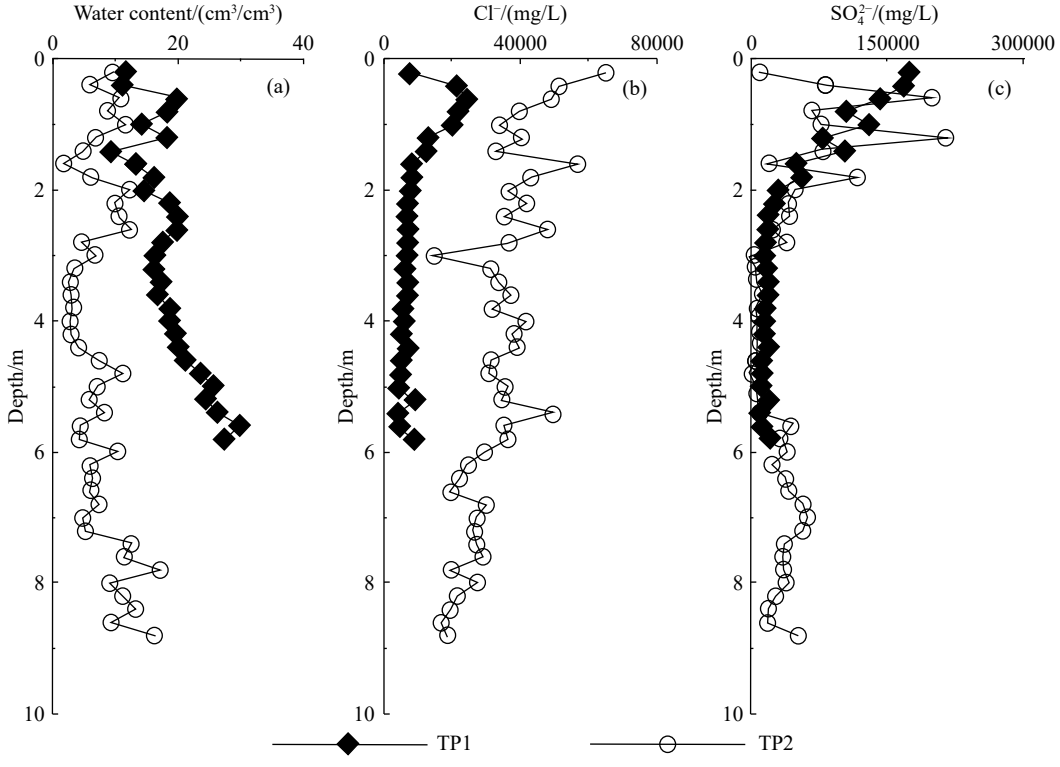

Fig. 6. Water content, chloride and sulfate concentrations of TP1 and TP2.

Table 4. Summary of weighted profile moisture contents, weighted solute concentrations, and total solute concentrations.

Profile	Moisture content/(cm^3/cm^3)			Cl^- concentration/(mg/ L)			Total Cl^- storage/(g/m^2)	SO_4^{2-} concentration/(mg/L)			Total SO_4^{2-} storage/(g/m^2)
	Mean	Min	Max	Mean	Min	Max		Mean	Min	Max	
TP1	18.7	9.4	29.7	9169.3	4279.2	24354.5	9861.2	46907.6	11004.1	175435.4	29533.9
TP2	7.7	1.8	17.0	33904.7	14548.5	64989.1	28762.7	41372.3	3417.0	214988.2	30696.7
TP3	17.9	5.8	33.7	300.9	74.1	1044.8	326.2	1297.5	234.2	6162.9	741.0
TP4	22.4	9.2	35.0	457.4	98.0	1079.0	822.5	2569.5	1187.1	6809.3	4072.6

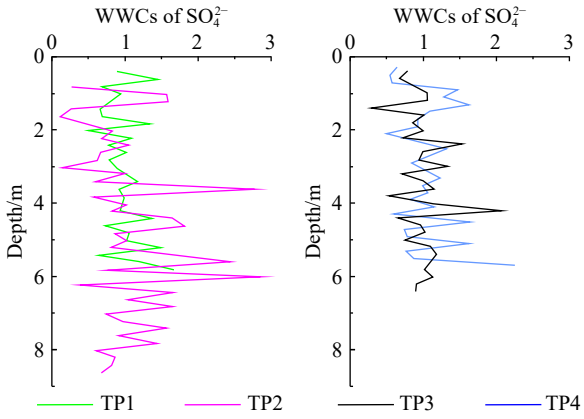

Fig. 7. Water washing coefficients of SO_4^{2-} in the four profiles.

extremely low (0.07 mm/a), which may result from the presence of clay in the upper 4 m, because previous studies indicate that variations in deep drainage are related to soil texture (Allison GB and Hughes MW, 1983; Kennett-Smith A et al., 1994; Keese KE et al., 2005; Wang T et al., 2009; Kim JH and Jackson RB, 2012). A modeling study shows that soil textural variability reduces recharge by factors of 2–11 (Keese KE et al., 2005) and clay contents in the upper soil profile can be used as a surrogate to regionalize deep drainage rates beneath cleared areas on the basis of high correlations between deep drainage and clay contents (Kennett-Smith A et al., 1994).

As croplands have the highest water input, including precipitation and irrigation, groundwater recharge is highest among croplands, grasslands, woodlands, and scrublands (Kim JH and Jackson RB, 2012). But, groundwater recharge under croplands is highly variable across the world. A mean average deep drainage rate for croplands is about 10.0 mm/a (0.1 mm/a to 50.0 mm/a) in southern Australia (Cook PG et al., 2001), while it is up to 205.0 mm/a for the irrigated farmland in Italy. Deep drainage rates have been estimated for approximately 50 profiles in China using the CMB method. For example, deep drainage rates for the irrigated farmlands range from 31.3 mm/a to 65.0 mm/a in the North China Plain (Wang BG et al., 2006) and from 47.0 mm/a to 50.0 mm/a in arid areas of Northwest China (Huang TM et al., 2013) respectively, which is similar to those at TP3 and TP4 (61.2 mm/a and 44.8 mm/a, respectively).

Groundwater recharge at natural lands and croplands in this study indicates that it increases dramatically after the conversion from the former to the latter, which has a good agreement with previous studies reporting the increase at one to two orders of magnitude (Allison GB and Hughes MW, 1983; Scanlon BR et al., 2006). There are two possible reasons. Firstly, the introduced irrigation water to meet the rainfall deficit increases the amount of potential water sources that can become groundwater. The amount of water applied using the traditional flooding irrigation may be comparable or exceed the annual precipitation (Wang BG, et al., 2008). Secondly, in (semi-) arid regions, native plans usually have deep roots to obtain deep soil moisture (Jackson RB et al., 1996), particularly trees that use both soil water and groundwater (Yin LH et al., 2013). Groundwater recharge will significantly increase after replacing with short-rooted crops that reduce evapotranspiration (Radford BJ et al., 2009). The

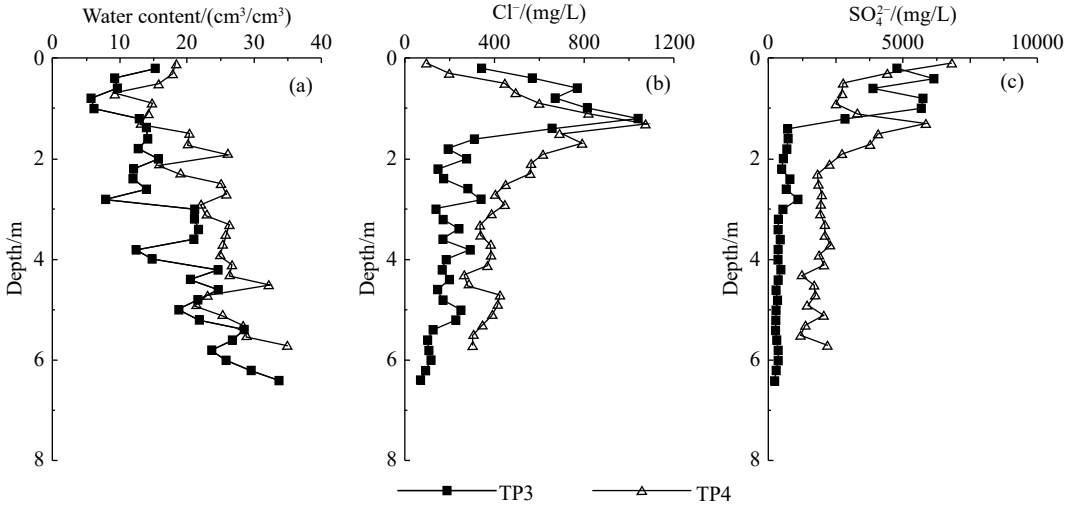

Fig. 8. Water content, chloride and sulfate of TP3 and TP4.

global analysis depicts that groundwater recharge will triple after the conversion of woodland to croplands under a water-limited condition (Kim JH and Jackson RB, 2012).

3.5. Implications for management

About 3.14×10^6 km^2 worldwide are irrigated croplands (Salmon JM et al., 2015). There are two types of irrigation, i.e., groundwater-fed (30%) and surface water-fed (70%) (Wada Y et al., 2014). In many arid regions, groundwater has been one of the major irrigation water sources and is expected to further increase due to overused surface and reduced reliability of precipitation. Although groundwater recharge in croplands increases after conversion, its amount is much lower than the pumping rate in most cases, which results in a continuous decline of the water table. For example, the water table in North China Plain and High Plains Aquifer in the United States has lowered more than 40 m due to groundwater pumping for irrigation (Cao GL et al., 2016; Lauffenburger ZH et al., 2018). In NW China, croplands are usually in the oasis-desert settings. The lowering of the water table will cause the dieback of phreatophytes in the edge of deserts and the spread of desertification, in addition to the depletion of groundwater resources. Due to water table decline, the belt width of *Tamarix* between the oasis and the desert decreases remarkably from 1000 m to about 30 m in inland basin of NW China (Ma JZ et al., 2009b).

For irrigation using surface water, the water table will rise significantly due to the increased groundwater recharge, which will result in serious soil salinization (Smedema LK and Shiati K, 2002). The total global area of salt-affected soils was 8.31×10^6 km^2, extending over all the continents including Africa, Asia, Australasia, and the Americas (Martinez-Beltran J and Manzur CL, 2005). In China, the total area of salinization is about 0.36×10^6 km^2, mainly in (semi-) arid regions, due to excessive irrigation (Li JG et al., 2014). Irrigation-induced recharge can increase the chemical load to the soil and mobilize the existing salt inventories accumulated during the geological history (McMahon PB et al., 2006; Robertson WM et al., 2015; Turkeltaub T et al., 2015), which degrades water quality. For instance, groundwater nitrate concentration increased by 0.7−0.9 mg/L over periods ranging from 10 years to over 50 years due to land-use changes (Robertson WM and Sharp JM., 2015). In the study, the deterioration of groundwater quality is not observed, which may be due to the small percentage of irrigation lands (about 10%). Groundwater quality degradation is expected under a scenario that large-scale cultivation occurs. For both groundwater- and surface water-fed irrigation, water-saving technologies should be applied to enhance water use efficiency to minimize the negative effect on soil and plants. Numerical modeling indicates that under drip irrigation, water use efficiency will be increased by up to 77% (Hu QL et al., 2017)

4. Conclusions

Regional aridity is increasing under global climate change, and therefore the sustainable use of water resources has drawn attention from scientists and the public. In this study, two tracer-based methods, i.e., chloride and sulfate, were applied to quantify groundwater recharge under different land use. In the natural lands, groundwater recharge is negligible, ranging from 0.07 mm/a to 0.40 mm/a. In contrast, groundwater recharge increase dramatically up to 44.80−61.20 mm/a after the conversion.

The estimated groundwater recharge indicates that the conversion of natural lands to croplands has resulted in substantial increases in groundwater recharge, indicating that land-use changes can significantly alter groundwater resources in a given region.

The study also suggests that the sulfate mass balance method yields result similar to that from the chloride mass balance method, indicating that sulfate can be used as an alternative tracer to quantify groundwater recharge in arid regions.

Acknowledgments

The research was funded by Innovation Capability Support Program of Shaanxi (2019TD-040), China National Natural Science Foundation (41472228, 41877199), Groundwater and Ecology Security in the North Slope Economic Belt of the Tianshan Mountain (201511047) and Key Laboratory of Groundwater and Ecology in Arid Regions of China Geological Survey.

References

Adane ZA, Gates JB. 2015. Determining the impacts of experimental forest plantation on groundwater recharge in the Nebraska Sand Hills (USA) using chloride and sulfate. Hydrogeology, 23(1), 81–94. doi: 10.1007/s10040-014-1181-6.

Allison GB, Hughes MW. 1983. The use of natural tracers as indicators of soil-water movement in a temperate semi-arid region. Journal of Hydrology, 60(1), 157–173. doi: 10.1016/0022-1694(83)90019-7.

Anderson VG. 1945. Some effects of atmospheric evaporation and transpiration on the composition of natural water in Australia (continued). Underground waters in riverless areas. Aust Chem Inst, 12, 83–98. doi: 10.1016/j.agwat.2018.04.016.

Cao GL, Scanlon BR, Han DM, Zheng CM. 2016. Impacts of thickening unsaturated zone on groundwater recharge in the North China Plain. Hydrogeology, 537, 260–270. doi: 10.1016/j.jhydrol.2016.03.049.

Chen ZY, Bi EP, Nie ZL, Ye H, Nan YJ. 2001. Tentative discussion on paleohydrological and paleoclimatical information from unsaturated zone profile. Acta Geoscientia Sinica, 22, 335–339.

Chen Z, Xu H. 1996. Chloride tracer method for estimation natural groundwater recharge in arid and semiarid regions. Geological Science and Technology Information, 15(3), 87–92.

Chen ZY, Zhang GH, Xu JM. 1998. Paleoclimate record deduced from groundwater and climate change implications of groundwater resources in North China. Bulletin of the Chinese Academy of Geological Sciences, 19(4), 338–345.

Cook PG, Edmunds WM, Gaye CB. 1992. Estimating palcorecharge and palcoclimate from unsaturated zone profiles. Water Resources Research, 28(12), 2721–2731. doi: 10.1029/92wr01298.

Cook PG, Leaney FW, Jolly ID. 2001. Groundwater recharge in the Mallee region, and salinity implications for the Murray River. Tech Rep, 45(1), CSIRO Land and Water, Acton, Australia.

Crosbie RS, Peeters LJ, Herron N, McVicar TR, Herr A. 2017. Estimating groundwater recharge and its associated uncertainty: Use of regression kriging and the chloride mass balance method. Journal of Hydrology, 561, 1063–1080. doi: 10.1016/j.jhydrol.2017.08.003.

Doell P, Mueller SH, Schuh C, Portmann FT, Eicker A. 2014. Global-scale assessment of groundwater depletion and related groundwater abstractions: Combining hydrological modeling with information from well observations and GRACE satellites. Water Resources Research, 50(3), 5698–5720. doi: 10.1002/2014wr015595.

Edmunds WM, Ma JZ, Aeschbach-Hertig W, Kipfer R, Darbyshire DPF. 2006. Groundwater recharge history and hydrogeochemical evolution in the Minqin Basin, North West China. Applied Geochemistry, 21(12), 2148–2170. doi: 10.1016/j.apgeochem.2006.07.016.

Federico AF, Geoff P. 2010. Local recharge processes in glacial and alluvial deposits of a temperate catchment. Journal of Hydrology, 389(1−2), 90–100. doi: 10.1016/j.jhydrol.2010.05.025.

Feng W, Zhong M, Lemoine JM, Biancale R, Hsu HT, Xia J. 2013. Evaluation of groundwater depletion in North China using the Gravity Recovery and Climate Experiment (GRACE) data and ground‐based measurements. Water Resources Research, 49(4), 2110–2118. doi: 10.1002/wrcr.20192.

Gates JB, Edmunds WM, Darling WG, Ma JZ, Pang ZH, Adam AY. 2008a. Conceptual model of recharge to southeastern Badain Jaran Desert groundwater and lakes from environmental tracers. Applied Geochemistry, 23(12), 3519–3534. doi: 10.1016/j.apgeochem.2008.07.019.

Gates JB, Edmunds WM, Ma JZ, Scanlon BR. 2008b. Estimating groundwater recharge in a cold desert environment in northern China using chloride. Hydrogeology, 16(5), 893–910. doi: 10.1007/s10040-007-0264-z.

Han D, Currell MJ, Cao G, Hall B. 2017. Alterations to groundwater recharge due to anthropogenic landscape change. Journal of Hydrology, 554, 545–557. doi: 10.1016/j.jhydrol.2017.09.018.

Harrington GA, Cook PG, Herczeg AL. 2002. Spatial and temporal variability of ground water recharge in central Australia: A tracer approach. Groundwater, 40(5), 518–527. doi: 10.1111/j.1745-6584.2002.tb02536.x.

Hu QL, Yang YH, Han SM, Yang YM, Ai ZP, Wang JS, Ma FY. 2017. Identifying changes in irrigation return flow with gradually intensified water-saving technology using HYDRUS for regional water resources management. Agricultural Water Management, 194(2), 33–47. doi: 10.1016/j.agwat.2017.08.023.

Huang TM, Pang ZH. 2011. Estimating groundwater recharge following land-use change using chloride mass balance of soil profiles: A case study at Guyuan and Xifeng in the Loess Plateau of China. HydrogeolJournal19,177–186.doi:http://377.rm.cglhub.com/10.1007/s10040–010-0643–8.

Huang TM, Pang ZH, Chen YN, Kong YL. 2013. Groundwater circulation relative to water quality and vegetation in an arid transitional zone linking oasis, desert and river. Chinese Science Bulletin. 58, 3088 –3097. doi: http://377.rm.cglhub.com/10.1007/s11434–013-5948–2.

Huang TM, Pang ZH, Liu J, Yin LH, Edmunds WM. 2017. Groundwater recharge in an arid grassland as indicated by soil chloride profile and multiple tracers. Hydrological Processes, 31(12), 1047–1057. doi: 10.1002/hyp.11089.

Jackson RB, Canadell J, Ehleringer JR, Mooney HA, Sala OE, Schulze ED. 1996. A global analysis of root distributions for terrestrial biomes. Oecologia, 108(3), 389–411. doi: 10.1007/bf00333714.

Keese KE, Scanlon BR, Reedy RC. 2005. Assessing controls on diffuse groundwater recharge using unsaturated flow modeling. Water Resources Research, 41(6), 1–6. doi: 10.1029/2004wr003841.

Kennett-Smith A, Cook PG, Walker GR. 1994. Factors affecting groundwater recharge following clearing in the south western Murray Basin. Journal of Hydrology, 154(1−4), 85–105. doi: 10.1016/0022-1694(94)90213-5.

Kim JH, Jackson RB. 2012. A global analysis of groundwater recharge for vegetation, climate, and soils. Vadose Zone, 11(1), 120–128. doi: 10.2136/vzj2011.0021.

Lauffenburger ZH, Gurdak JJ, Hobza C, Woodward D, Wolf C. 2018. Irrigated agriculture and future climate change effects on groundwater recharge, northern High Plains aquifer, USA. Agricultural Water Management, 204, 69–80. doi: 10.1016/j.agwat.2018.03.022.

Li JG, Pu LJ, Han MF, Zhu M, Zhang RS, Xiang YZ. 2014. Soil salinization research in China: Advances and prospects. Journal of Geographical Sciences, 24(5), 943–960. doi: 10.1007/s11442-014-1130-2.

Liu XY, Chen JS, Sun XS. 2010. Application of chloride tracer method to study replenishment ratio of precipitation in desert. Transactions of the CSAE, 26(s1), 146–149. doi: 10.1109/icetce.2011.5774776.

Ma JZ, Li X, Huang TM, Edmunds WM. 2005. Chemical Evolution and Recharge Characteristics of Water Resources in the Shiyang River Basin. Resources Science, 27(3), 117–122. doi: 10.1016/j.jenvman.2008.05.007.

Ma JZ, Ding ZY, Edmunds WM, Gates JB, Huang TM. 2009a. Limits to recharge of groundwater from Tibetan plateau to the Gobi desert, implications for water management in the mountain front. Journal of Hydrology, 364(2), 128–141. doi: 10.1016/j.jhydrol.2008.10.010.

Ma JZ, Ding ZY, Wei GX, Zhao H, Huang TM. 2009b. Sources of water pollution and evolution of water quality in the Wuwei basin of Shiyang river, Northwest China. Journal of Environmental Management, 90(2), 1168–1177. doi: 10.1016/j.jenvman.2008.05.007.

Ma QL, Wang JH, Li XR, Zhu SJ, Liu HJ, Zhan KJ. 2009. Long-term changes of Tamarix-vegetation in the oasis-desert ecotone and its driving factors: Implication for dryland management. Environmental Earth Sciences, 59, 765. doi: 10.1007/s12665-009-0072-y.

Martinez-Beltran J, Manzur CL. 2005. Overview of salinity problems in the world and FAO strategies to address the problem. Proceedings of the International Salinity Forum, Riverside, California, April 2005, 311–313.

McMahon PB, Dennehy KF, Bruce BW, Böhlke JK, Michel RL, Gurdak JJ, Hurlbut DB. 2006. Storage and transit time of chemicals in thick unsaturated zones under rangeland and irrigated cropland, High Plains, United States. Water Resources Research, 42(3), 1–3. doi: 10.1029/2005wr004417.

Nian YY, Li X, Zhou J, Hu XL. 2014. Impact of land use change on water resource allocation in the middle reaches of the Heihe River Basin in northwestern China. Journal of Arid Land, 6(3), 273–286. doi: 10.1007/s40333-013-0209-4.

Perera N, Gharabaghi B, Howard K. 2013. Groundwater chloride response in the Highland Creek watershed due to road salt application: A re-assessment after 20 years. Journal of Hydrology, 479(1), 159–168. doi: 10.1016/j.jhydrol.2012.11.057.

Radford BJ, Silburn DM, Forster BA. 2009. Soil chloride and deep drainage responses to land clearing for cropping at seven sites in central Queensland, northern Australia. Journal of Hydrology, 379, 20–29. doi: 10.1016/j.jhydrol.2009.09.040.

Robertson WM, Sharp JM. 2015. Estimates of net infiltration in arid basins and potential impacts on recharge and solute flux due to land use and vegetation change. Journal of Hydrology, 522(3), 211–227. doi: 10.1016/j.jhydrol.2014.11.081.

Russo SL, Zavattaro L, Acutis M, Zuppi GM. 2003. Chloride profile technique to estimate water movement through unsatured zone in a cropped area in subhumid climate(Po Valley-NW Italy). Journal of Hydrology, 270(1−2), 65–74. doi: 10.1016/s0022-1694(02)00278-0.

Salmon JM, Friedl MA, Frolking S, Wisser D, Douglas EM. 2015. Global rain-fed, irrigated, and paddy croplands: A new high resolution map derived from remote sensing, crop inventories and climate data. International Journal of Applied Earth Observation and Geoinformation, 38(6), 321–334. doi: 10.1016/j.jag.2015.01.014.

Scanlon BR, Keese KE, Flint AL, Flint LE, Gaye CB, Edmunds WM, Simmers I. 2006. Global synthesis of groundwater recharge in semiarid and arid regions. Hydrological Process, 20(15), 3335–3370. doi: 10.1002/hyp.6335.

Scanlon BR, Faunt CC, Longuevergne L, Reedy RC, Alley WM, McGuire VL, McMahon PB. 2012. Groundwater depletion and sustainability of irrigation in the US High Plains and Central Valley. Proceedings of the National Academy of Sciences, 109(2), 9320–9325. doi: 10.1073/pnas.1200311109.

Scanlon BR, Healy RW, Cook PG. 2002. Choosing appropriate techniques for quantifying groundwater recharge. Hydrogeology

Journal, 10(2), 18–39. doi: 10.1007/s10040-002-0200-1.
Scanlon BR, Reedy RC, Tachovsky JA. 2007. Semiarid unsaturated zone chloride profiles: Archives of past land use change impacts on water resources in the southern High Plains, United States. Water Resources Research, 43(6), 1–13. doi: 10.1029/2006wr005769.
Scanlon BR, Reedy RC, Stonestrom DA, Prudic DE, Dennehy KF. 2005. Impact of land use and land cover change on groundwater recharge and quality in the southwestern US. Global Change Biology, 11(10), 1577–1593. doi: 10.1111/j.1365-2486.2005.01026.x.
Scanlon BR, Gates JB, ReedyRC, Jackson WA, Bordovsky JP. 2010. Effects of irrigated agroecosystems: 2. Quality of soil water and groundwater in the southern High Plains, Texas. Water Resources Research, 46, 9. doi: 10.1029/2009WR008427.
Schmidt S, Geyer T, Marei A, Guttman J, Sauter M. 2013. Quantification of long-term wastewater impacts on karst groundwater resources in a semi-arid environment by chloride mass balance methods. Journal of Hydrology, 502(10), 177–190. doi: 10.1016/j.jhydrol.2013.08.009.
Selaolo ET. 1998. Tracer studies and groundwater recharge assessment in the eastern fringe of the Botswana Kalahari, Ph. D. thesis, Freie Univ., Amsterdam, Netherlands.
Simmers I. 2013. Estimation of Natural Groundwater Recharge. Eos Transactions American Geophysical Union, 70, 131. doi: 10.1029/89EO00076.
Smedema LK, Shiati K. 2002. Irrigation and salinity: A perspective review of the salinity hazards of irrigation development in the arid zone. Irrigation and Drainage Systems, 16(2), 161–174. doi: 10.1023/A:1016008417327.
Stone WJ. 1992. Paleohydrologic implications of some deep soilwater chloride profiles, Murray Basin, South Australia. Journal of Hydrology, 132(1−4), 201–223. doi: 10.1016/0022-1694(92)90179-Y.
Taiz L, Zeiger E. 2010. Plant physiology (fifth edition). U.S.A, Sinauer Assosiates Inc., 310−312.
Tilman D, Balzer C, Hill J, Befort BL. 2011. Global food demand and the sustainable intensification of agriculture. Proceedings of the National Academy of Sciences, 108(50), 20260–20264. doi: 10.1073/pnas.1116437108.
Tolmie PE, Silburn DM, Biggs AJW. 2011. Deep drainage and soil salt loads in the Queensland Murray-Darling Basin using soil chloride: Comparison of land uses. Soil Research, 49(5), 408–423. doi: 10.1071/sr10172.
Torres EA, Calera A. 2010. Bare soil evaporation under high evaporation demand: A proposed modification to the FAO-56 model. Hydrological Sciences Journal, 55(3), 303–315. doi: 10.1080/02626661003683249.
Turkeltaub T, Kurtzman D, Russak EE, Dahan O. 2015. Impact of switching crop type on water and solute fluxes in deep vadose zone. Water Resources Research, 51(12), 9828–9842. doi: 10.1002/2015wr017612.
Tyler SW, Chapman JB, Conrad SH, Hammermeister DP, Blout DO, Miller JJ, Sully MJ, Ginanni JM. 1996. Soil-water flux in the southern Great Basin, United States: Temporal and spatial variations over the last 120,000 years. Water Resources Research, 32(6), 1481–1499. doi: 10.1029/96wr00564.
Wada Y, Wisser D, Bierkens MFP. 2014. Global modeling of withdrawal, allocation and consumptive use of surface water and groundwater resources. Earth System Dynamics Discussions, 5(1), 15–40. doi: 10.5194/esd-5-15-2014.
Wang YG, Xiao DN, Li Y. 1993. Spatial and temporal dynamics of Oasis soil salinization in upper and middle reaches of Sangonghe River, Northwest China. Journal of Desert Research, 28(3), 478–484. doi: 10.1127/lr/9/1993/1.
Wang BG, Jin MG, Wang WF, Yang L. 2006. Application of chloride Ion tracer method in estimation of vertical infiltration recharge of groundwater in Hebei Plain. Water Saving Irrigation, 3(3), 16–20.
Wang BG, Jin MG, Nimmo JR, Yang L, Wang WF. 2008. Estimating groundwater recharge in Hebei Plain, China under varying land use practices using tritium and bromide tracers. Journal of Hydrology, 356(1−2), 209–222. doi: 10.1016/j.jhydrol.2008.04.011.
Wang Q, Shen YJ, Pei HW, Tian HY, Li F, Pei YS. 2013. Dynamic characteristics and drainage assessment of deepsoil moisture in the irrigated farmland of piedmont region of North China plain. South-to-North Water Transfers and Water Science & Technology, 11(1), 155–160. doi: 10.3724/SP.J.1201.2013.01155.
Wang T, Istanbulluoglu E, Lenters J, Scott D. 2009. On the role of groundwater and soil texture in the regional water balance: An investigation of the Nebraska Sand Hills, USA. Water Resources Research, 45, 82–90. doi: 10.1029/2009wr007733.
Wei J, Liu ZH, Zhao LL. 2011. Analysis on the annual chemical composition in Urumqi. Journal of Xinjiang University (Natural Science Edition), 28(3), 278–282 (in Chinese with English abstract). doi: 10.3969/j.issn.1000-2839.2011.03.004.
Wood WW. 1999. Use and misuse of the chloride‐mass balance method in estimating ground water recharge. Groundwater, 37(1), 2–3. doi: 10.1111/j.1745-6584.1999.tb00949.x.
Yan HM, Liu JY, Huang HQ, Tao B, Cao MK. 2009. Assessing the consequence of land use change on agricultural productivity in China. Global and Planetary Change, 67(1−2), 13–19. doi: 10.1016/j.gloplacha.2008.12.012.
Yin LH, Hu GC, Huang JT, Wen DG, Dong JQ, Wang XY, Li HB. 2011. Groundwater-recharge estimation in the Ordos Plateau, China: Comparison of methods. Hydrogeology, 19(8), 1563–1575. doi: 10.1007/s10040-011-0777-3.
Yin LH, Huang JT, Wang XY, Dong JQ, Ma HY, Zhang J. 2013. Characteristics of night time sap flow of Salix matsudana and Populus simonii in Yulin, Shaanxi. Journal of Northwest Sci-Tech University of Agriculture and Forestry, 41(8), 85–90.
Yin LH, Zhou YX, Huang JT, Wenninger J, Zhang E, Hou GC, Dong JQ. 2015. Interaction between groundwater and trees in an arid site: Potential impacts of climate variation and groundwater abstraction on trees. Journal of Hydrology, 528(9), 435–448. doi: 10.1016/j.jhydrol.2015.06.063.
Zhang N, Kang YQ, Liu XW, Bai L. 1999. Investigation and study on background value of natural dustfall in Gansu. Environmental Research and Monitoring in Gansu, 12(5), 69–73.
Zhang GF, Fei YH, Wang JZ, Chen ZY, Nie ZL. 2003. Evolution characteristics and trend of shallow groundwater recharge in Taihangshan Piedmont Plain over the last 300 years. Acta Geoscientia Sinica, 24(10), 261–266. doi: 10.3321/j.issn:1006-3021.2003.03.011.
Zhang Q, Luo GY, Li LH, Zhang M, Lv NN, Wang XX. 2017. An analysis of oasis evolution based on land use and land cover change: A case study in the Sangong River Basin on the northern slope of the Tianshan Mountains. Journal of Geographical Sciences, 27(2), 223–229. doi: 10.1007/s11442-017-1373-9.
Zhang ZH, Shi DH, Shen ZL, Xue YQ. 1997. Evolution and development of groundwater environment in North China Plain under human activities. Bulletin of the Chinese Academy of Geological Sciences, 18(4), 337–344.
Zhu GF, Li ZZ, Su YH, Ma JZ, Zhang YY. 2007. Hydrogeochemical and isotope evidence of groundwater evolution and recharge in Minqin Basin, Northwest China. Journal of Hydrology, 333(2−4), 239–251. doi: 10.1016/j.jhydrol.2006.08.013.
Zuo LJ, Zhang ZX, Carlson KM, MacDonald GK, Brauman KA, Liu YC, Zhang W, Zhang HY, Wu WB, Zhao XL, Wang X, Liu B, Yi L, Wen QK, Liu F, Xu JY, Hu SG, Sun FF, Gerber JS, West PC. 2018. Progress towards sustainable intensification in China challenged by land-use change. Nature Sustainability, 1(6), 304–313. doi: 10.1038/s41893-018-0076-2.